Spin Dynamics and Andreev-Bashkin Effect in Mixtures of One-Dimensional Bose Gases

L. Parisi,[1] G. E. Astrakharchik,[2] and S. Giorgini[1]

[1]*Dipartimento di Fisica, Università di Trento and CNR-INO BEC Center, I-38050 Povo, Trento, Italy*
[2]*Departament de Física i Enginyeria Nuclear, Universitat Politècnica de Catalunya,
Campus Nord B4-B5, E-08034 Barcelona, Spain*

We investigate the propagation of spin waves in two-component mixtures of one-dimensional Bose gases interacting through repulsive contact potentials. By using quantum Monte Carlo methods we calculate static ground-state properties, such as the spin susceptibility and the spin structure factor, as a function of the coupling strengths and we determine the critical parameters for phase separation. In homogeneous mixtures, results of the velocity of spin waves and of its softening close to the critical point of phase separation are obtained by means of hydrodynamic theory and a sum-rule approach. We quantify the nondissipative drag effect, resulting from the Andreev-Bashkin current-current interaction between the two components of the gas, and we show that in the regime of strong coupling it causes a significant suppression of the spin-wave velocity.

The problem of dissipationless spin transport is a widely studied topic in condensed matter physics with important applications to electron-hole superfluidity, superfluid ^{3}He, and spintronic devices [1]. Ultracold gases, with the possibility they offer to realize quantum degenerate mixtures, open new interesting perspectives for the investigation of spin dynamics. Spin diffusion in a strongly interacting two-component Fermi gas has been observed and characterized in a series of recent experiments [2–4], whereas the existence of spin supercurrents in Bose mixtures has been demonstrated both at very low temperatures [5–10] and in the presence of a large thermal component [11]. In this respect one-dimensional (1D) mixtures are particularly interesting for several reasons: (i) the low-energy dynamics is universal and described by the Luttinger liquid model [12]; (ii) spin and charge degrees of freedom are expected to be completely decoupled at low energy [13,14]; and, finally, (iii) regimes of strong interactions can be achieved in long-lived samples [15–18].

The undamped propagation of spin waves is an important signature of spin superfluidity and an unbiased determination of the spin-sound velocity is a crucial element to understand the dynamics of two-component Bose mixtures at ultralow temperatures. Notably, for such mixtures, the propagation of sound in the spin channel depends not only on the static magnetic susceptibility, but also on a purely dynamic quantity known as the Andreev-Bashkin nondissipative drag [19]. This intriguing effect, never observed so far, involves two coupled superfluids and entails that a superflow in one component can induce a supercurrent in the second component which is dragged without energy dissipation. In its original form, the Andreev-Bashkin effect was discussed in connection with possible superfluid mixtures of ^{3}He in ^{4}He. However, due to the limited solubility of the two isotopes [20], such superfluid mixtures have never been realized. In the context of ultracold atoms the Andreev-Bashkin effect was studied in the continuum using a perturbative approach based on the Bogoliubov theory [21] as well as in lattice systems [22]. More recently, its consequences on the propagation of spin waves were analyzed using the hydrodynamic theory [23].

In the present work we investigate spin dynamics and the effect of the Andreev-Bashkin superfluid drag in 1D repulsive mixtures of Bose gases. To this aim we use quantum Monte Carlo (QMC) methods first to establish the critical condition for the miscibility of the two gases, which is a preliminary requisite to investigate the regime of homogeneous mixtures. Second, we calculate the entrainment effect from the coupled superfluid response and the spin-wave velocity by means of hydrodynamic theory and of a sum-rule approach. On the basis of simulations performed by varying both the intraspecies and the interspecies coupling strength, we find that the superfluid drag can be large if the interspecies coupling is strong, and it contributes to the softening of spin waves on approaching the critical point of phase separation.

We consider Bose-Bose mixtures in a 1D geometry described by the following Hamiltonian:

$$H = -\frac{\hbar^2}{2m}\sum_{i=1}^{N_a}\frac{\partial^2}{\partial x_i^2} + g\sum_{i<j}\delta(x_i - x_j) - \frac{\hbar^2}{2m}\sum_{\alpha=1}^{N_b}\frac{\partial^2}{\partial x_\alpha^2}$$
$$+ g\sum_{\alpha<\beta}\delta(x_\alpha - x_\beta) + \tilde{g}\sum_{i,\alpha}\delta(x_i - x_\alpha), \quad (1)$$

which includes, in addition to the kinetic energy terms of the two components with N_a and N_b particles, equal intraspecies interactions modeled by the contact coupling

constant $g > 0$ and a contact interspecies repulsive potential of strength $\tilde{g} > 0$. Here x_i with $i = 1, \ldots, N_a$ and x_α with $\alpha = 1, \ldots, N_b$ denote, respectively, the positions of particles belonging to component a and b of the mixture. We also consider mass balanced mixtures, m being the mass of particles of both components. In the absence of interspecies interactions, the above Hamiltonian for each component separately yields the well-known Lieb-Liniger (LL) model [24], which can be solved exactly via the Bethe ansatz for any value of the coupling constant g. In particular, for very strong repulsion ($g \to \infty$) corresponding to the so-called Tonks-Girardeau (TG) regime, the LL model describes a gas of impenetrable bosons which is equivalent to a gas of noninteracting spinless fermions [25]. The full Hamiltonian, Eq. (1), consists of two LL gases, with the same interaction strength g, coupled via a contact repulsive force. One should point out that this full Hamiltonian also admits exact solutions, but only when it enjoys SU(2) symmetry, i.e., if $\tilde{g} = g$ or when both components are in the TG regime ($g = \infty$). In the first case the ground state is ferromagnetic [26,27] and the equation of state can be calculated using the LL model of a single-component gas. In the latter case, the system corresponds to a mixture of interacting Fermi gases and the solution is provided by the Yang-Gaudin model [28,29] yielding a paramagnetic ground state for any value of the repulsive coupling $\tilde{g}$. In all other cases, for which the Bethe ansatz approach is no longer applicable, only numerical solutions are available by means, for example, of QMC methods.

A population balanced system, where $N_a = N_b = N/2$, can be fully characterized in the thermodynamic limit by the following two dimensionless parameters:

$$\gamma = \frac{gm}{\hbar^2 n} \qquad \eta = \frac{\tilde{g}m}{\hbar^2 n}. \qquad (2)$$

These are fixed by the values of interaction strength and by the total density $n = n_a + n_b$ of the gas, where $n_a = N_a/L$ and $n_b = N_b/L$ are the densities of the two components in terms of the size L of the 1D box. In unbalanced configurations, an additional parameter is needed to describe the polarization: $P = (n_a - n_b)/n$. In Refs. [30,31] the ground-state energy of the Hamiltonian, Eq. (1), was calculated in the extreme case of one impurity immersed in a LL gas ($N_b = 1$). Here we make use of a similar diffusion Monte Carlo method extended to any configuration $N_b \leq N_a$ with periodic boundary conditions. This technique provides exact results for the ground-state energy $E(\gamma, \eta, P)$ of the mixture within statistical uncertainty [32]. More in detail, simulations utilize a guiding wave function used for importance sampling and to encode the contact boundary conditions imposed by the δ-function potentials in the Hamiltonian Eq. (1). The guiding wave function is constructed as a product of pairwise correlation terms which, at short interparticle distance, reproduce the exact solution of

the two-body problem with the contact potential, as well as many-body correlations typical of Luttinger liquids at longer distances [33]. In this way, unbiased calculations of properties of the interacting gas are actually carried out by simulating free particles subject to proper boundary conditions [30,34]. The relevance of finite-size effects is estimated by repeating the simulations with increasing numbers of particles (typically ranging from $N = 50$ to $N = 200$), thereby ensuring a well-controlled approach to the thermodynamic limit.

Phase separation.—The first question we address concerns the condition of miscibility of the mixture at $T = 0$ and of its eventual phase separation. This latter is signaled by the divergence of the magnetic susceptibility χ, whose inverse is related to the curvature of the energy increase as the system is polarized away from the $P = 0$ balanced configuration: $(1/\chi) = [(\partial^2 E/L)/(n^2 \partial P^2)]$. In the weak-coupling regime, corresponding to $\gamma \ll 1$ and $\eta \ll 1$, one can use the mean-field theory yielding the analytical result $(1/\chi) = [(g - \tilde{g})/2]$ [35]. Based on this approach the mixture is miscible for $\tilde{g} < g$ and phase separation occurs as soon as $\tilde{g} > g$. Furthermore, in the Yang-Gaudin model where both components are in the fermionic TG limit, the homogenous mixture is known to be stable for any value of the interspecies coupling strength $\tilde{g}$. A question worth addressing concerns the determination of the critical parameter for phase separation in the regime of intermediate values of the coupling strength γ. To this purpose we calculate the ground-state energy for fixed values of γ and η with varying polarization P. The characteristic dependencies, obtained for $\gamma = 2$ and $\gamma = 20$, are shown in Fig. 1. We find that the energy of the $P = 0$ state is lower than the one of the fully polarized ($P = 1$) state provided that $\eta < \gamma$. For η slightly larger than γ the energy lies above the $P = 1$ threshold signaling the instability against the formation of two fully polarized domains [36]. From the equation of state as a function of the polarization P we extract the inverse magnetic susceptibility $1/\chi$ which we report in Fig. 2 for various values of γ. We see that for $\gamma = 0.04$ the results of $1/\chi$ are well reproduced by the mean-field prediction whereas, for larger values of γ, deviations are visible away from the critical point. Close to the point of phase separation, however, we notice that the susceptibility of both $\gamma = 2$ and $\gamma = 20$ is well described by the linear dependence $1/\chi \propto (\gamma - \eta)$ of the mean-field prediction. Finally, for $\gamma = \infty$, our results reproduce the η dependence of $1/\chi$ obtained from the exact solution [37–39] of the Yang-Gaudin model at finite polarization [40]. From this analysis we conclude that, for the reported values of $\gamma < \infty$, the critical parameter for phase separation is $\eta = \gamma$. At this value of the interspecies interaction strength the system jumps from being paramagnetic with $P = 0$ to fully ferromagnetic. These results are consistent with the known findings of the Yang-Gaudin model ($\gamma = \infty$) where phase separation never occurs [28], and
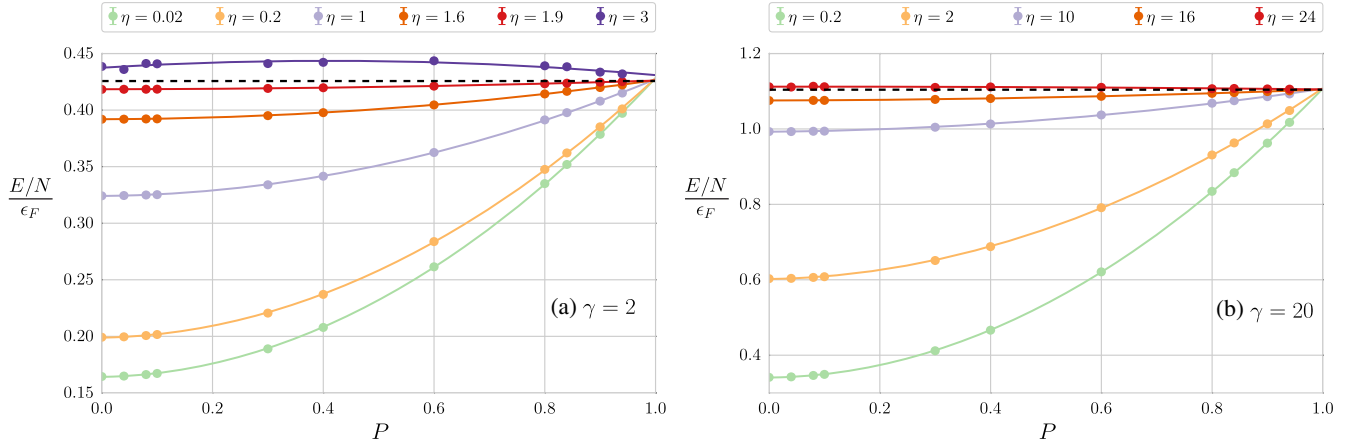
FIG. 1. Energy per particle of the homogeneous mixture as a function of the polarization P for different values of the coupling strengths η. Panel (a) refers to $\gamma = 2$ and panel (b) to $\gamma = 20$. Energies are shown in units of $\epsilon_F = [(\hbar^2 \pi^2 n^2)/(8m)]$ corresponding to the Fermi energy of the mixture when $\gamma = \infty$. The solid lines are best fits quadratic in P and the dashed horizontal lines indicate the energy of the fully polarized ($P = 1$) states. Statistical error bars are smaller than the symbol size.

of the SU(2) symmetric case ($\gamma = \eta$) where the stable phase is ferromagnetic [26,27].

Superfluid drag.—In a mixture of two superfluids with mass density ρ_1 and ρ_2, the energy change per unit volume due to finite superfluid velocities $\mathbf{v}_1$ and $\mathbf{v}_2$ is given by $\delta E = [(\rho_1 - \rho_D)v_1^2 + (\rho_2 - \rho_D)v_2^2 + 2\rho_D \mathbf{v}_1 \cdot \mathbf{v}_2]/2$. The quantity ρ_D accounts for the coupling between the superfluids and gives rise to a drag in the superfluid current density of each component: $\mathbf{j}_{1,2} = \partial \delta E / \partial \mathbf{v}_{1,2} = (\rho_{1,2} - \rho_D)\mathbf{v}_{1,2} + \rho_D \mathbf{v}_{2,1}$, known as the Andreev-Bashkin
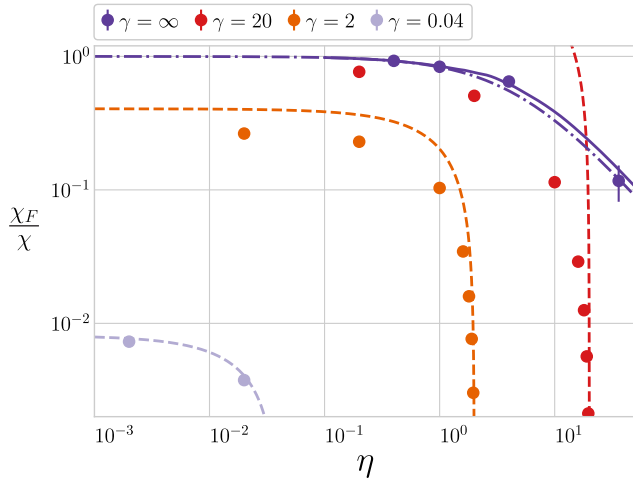

FIG. 2. Inverse susceptibility $1/\chi$ as a function of η for various values of γ ranging from the weak-coupling regime ($\gamma = 0.04$) to the TG limit ($\gamma = \infty$). Here $\chi_F = [(4m)/(\hbar^2 \pi^2 n)]$ is the susceptibility of the noninteracting mixture when $\gamma = \infty$. Dashed lines correspond to the mean-field result $1/\chi = (g - \tilde{g})/2$, whereas the dash-dotted line to the perturbation expansion $(\chi_F/\chi) = 1 - (2\eta/\pi^2)$ holding in the TG limit. The solid line is obtained from the exact solution of the Yang-Gaudin model at finite polarization.
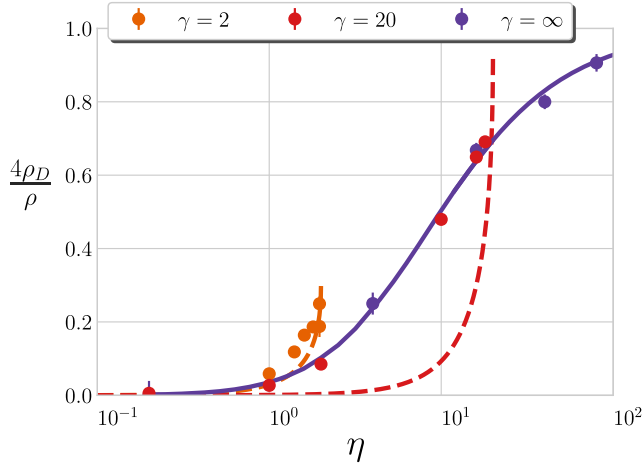
effect [19]. For 1D mixtures with $\rho_1 = \rho_2 = \rho/2$, one can calculate ρ_D to lowest order in $\tilde{g}$ by using the Bogoliubov approach of Ref. [21] which yields the result

$$\frac{\rho_D}{\rho} \simeq \frac{4\eta^2}{3\pi} \frac{1}{\left(\sqrt{2(\gamma + \eta)} + \sqrt{2(\gamma - \eta)}\right)^3}. \quad (3)$$

This shows that the drag effect is quadratic in the interspecies coupling η and is maximum at the critical point $\eta = \gamma$ where it takes the value $(\rho_D/\rho) = (\sqrt{\gamma}/6\pi)$. For arbitrary coupling strengths, we calculate ρ_D by means of the exact relation

$$4\frac{\rho_D}{\rho} = 1 - \lim_{\tau \to \infty} \frac{\langle [W_a(\tau) - W_b(\tau)]^2 \rangle}{4ND\tau}, \quad (4)$$

based on the paired superfluid response of the two components which in QMC simulations is provided by the statistics of winding numbers [23]. Here, $D = \hbar^2/2m$ is the diffusion constant of a free particle in imaginary time $\tau = it/\hbar$, whereas the winding number $W_a(\tau) = \sum_{i=1}^{N_a} \int_0^\tau d\tau' \{[dx_i(\tau')]/(d\tau')\}$ of the first component and, analogously, $W_b(\tau)$ of the second component are obtained by integrating the corresponding particle trajectories. In the absence of interspecies coupling, the winding numbers W_a and W_b are independent and, being normalized as $N_{a(b)} = \lim_{\tau \to \infty} [\langle W_{a(b)}^2(\tau) \rangle/(4D\tau)]$, result in $\rho_D = 0$. In the opposite case of fully paired motion of the two components, the relative winding number $(W_a - W_b)$ vanishes and the drag takes its maximum value $4\rho_D/\rho = 1$. In Fig. 3 we report the results of ρ_D calculated as a function of η for different values of the interaction parameter γ. We find that $4\rho_D/\rho$ approaches unity in the simultaneous limit $\gamma = \infty$ and

FIG. 3. Superfluid drag as a function of η for different values of γ. Dashed lines correspond to the weak-coupling result (3) for $\gamma = 2$ and $\gamma = 20$. The solid line refers to $\gamma = \infty$ and is obtained by inverting Eq. (5) with both χ and v_s from the exact solution of the Yang-Gaudin model.

$\eta = \infty$. However, already for $\gamma = 20$, ρ_D reaches ~ 0.7 of its maximum value in the vicinity of the critical point $\eta = \gamma$.

Velocity of spin waves.—Within the mean-field approach the long-wavelength elementary excitations in the spin channel consist of waves propagating with the velocity $v_s = \sqrt{\{[n(g - \tilde{g})]/(2m)\}}$ [35], such that $v_s^2 = [\rho/(m^2\chi)]$ in terms of the magnetic susceptibility and of the mass density $\rho = mn$. This result, however, holds only if one neglects the drag effect exerted by one component as it moves with respect to the other. More generally, the hydrodynamic model accounting for the Andreev-Bashkin effect yields the result [23]

$$v_s^2 = \frac{\rho - 4\rho_D}{m^2\chi}, \tag{5}$$

which involves the superfluid drag density ρ_D.

In order to determine the spin-wave velocity v_s, we follow two independent approaches. The first is based on the hydrodynamic theory of superfluids entailed by Eq. (5), where we determine v_s from knowledge of the magnetic susceptibility χ and of the superfluid drag ρ_D calculated above. The second, instead, is based on linear response theory and is conveniently discussed in terms of the frequency-weighted moments $m_k = \int d\omega (\hbar\omega)^k S_s(\mathbf{q}, \omega)$ of the spin-dependent dynamic structure factor $S_s(\mathbf{q}, \omega)$ [44]. In particular, for the following two moments one finds:

$$m_{-1} = N \frac{\chi_s(q)}{2n} \xrightarrow{q \to 0} N \frac{\chi}{2n}, \tag{6}$$

$$m_0 = S_s(q). \tag{7}$$

Here, Eq. (6) is the susceptibility sum rule involving the static spin-spin response function $\chi_s(q)$, which reduces to χ in the long-wavelength limit, and Eq. (7) defines the static spin-spin structure factor. One can show that in the $q \to 0$ limit both the m_{-1} and m_0 sum rules are exhausted by the spin-wave excitation with energy $\epsilon_s(q) = v_s\hbar q$, because multimode excitations contribute to the two sum rules with higher powers of q [45–48]. From this analysis it follows that the energy of the low-lying spin-wave excitations can be obtained from the ratio of sum rules calculated in the $q \to 0$ limit

$$\hbar q v_s = \lim_{q \to 0} \frac{m_0}{m_{-1}}. \tag{8}$$

A direct calculation of the static spin-spin structure factor $S_s(q)$ allows one to extract the coefficient of its low-q linear dependence $S_s(q)/N = [(v_s\chi)/(2n)]\hbar q$. Once divided by the magnetic susceptibility χ obtained above, this result gives the spin velocity v_s.

Both the hydrodynamic and the more microscopic estimate of v_s are shown in Fig. 4 and are found to agree within statistical errors providing very strong evidence of the reliability of our results. When $\gamma = \infty$ we also find agreement with the exact result of v_s from the Yang-Gaudin model [38,43]. By increasing the interspecies interaction strength, the spin-wave velocity decreases due to the combined effect of the susceptibility, which rises from the noninteracting value χ_0, and of the drag density ρ_D until it vanishes at the critical point of phase separation. For example, for $\eta = 10$ and $\gamma = 20$ the spin-wave velocity is reduced to $v_s \simeq 0.3 v_s^0$ of the value corresponding to $\eta = 0$
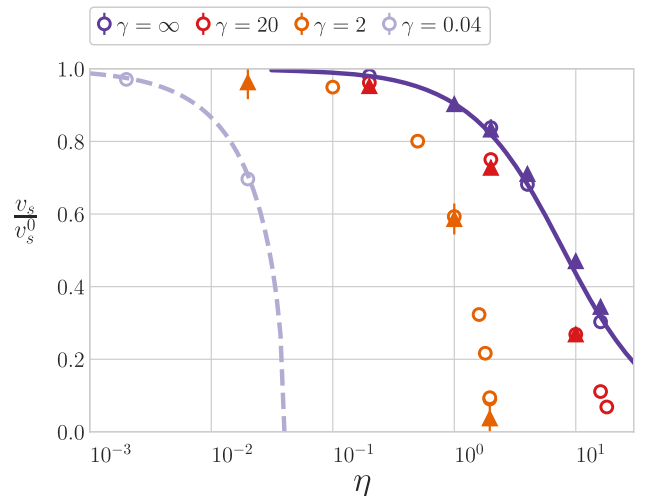

FIG. 4. Spin-wave velocity v_s as a function of η for different values of γ. The units are provided by the spin-wave velocity in the absence of interspecies interactions, $v_s^0 = \sqrt{\rho/m^2\chi_0}$. Open symbols refer to Eq. (5) and solid symbols to Eq. (8). The dashed line corresponds to the mean-field prediction $v_s = \sqrt{n(g - \tilde{g})/2m}$ and the solid line to the exact solution in the Yang-Gaudin model [38].

(see Fig. 4). The reduction is caused by an approximate fivefold increase of χ/χ_0 shown in Fig. 2 and by an additional factor of about 0.5 deriving from the term $1 - 4\rho_D/\rho$ shown in Fig. 3.

In conclusion, we provide exact predictions for the velocity of spin waves in repulsive 1D Bose mixtures. These results show the strong effect of the Andreev-Bashkin superfluid drag, which could be experimentally observed by means of independent measurements of the spin-wave velocity and of the magnetic susceptibility.

[1] E. Sonin, Adv. Phys. **59**, 181 (2010).
[2] A. Sommer, M. Ku, G. Roati, and M. W. Zwierlein, Nature (London) **472**, 201 (2011).
[3] A. B. Bardon, S. Beattie, C. Luciuk, W. Cairncross, D. Fine, N. S. Cheng, G. J. A. Edge, E. Taylor, S. Zhang, S. Trotzky, and J. H. Thywissen, Science **344**, 722 (2014).
[4] G. Valtolina, F. Scazza, A. Amico, A. Burchianti, A. Recati, T. Enss, M. Inguscio, M. Zaccanti, and G. Roati, Nat. Phys. **13**, 704 (2017).
[5] G. Modugno, M. Modugno, F. Riboli, G. Roati, and M. Inguscio, Phys. Rev. Lett. **89**, 190404 (2002).
[6] K. M. Mertes, J. W. Merrill, R. Carretero-González, D. J. Frantzeskakis, P. G. Kevrekidis, and D. S. Hall, Phys. Rev. Lett. **99**, 190402 (2007).
[7] E. Nicklas, H. Strobel, T. Zibold, C. Gross, B. A. Malomed, P. G. Kevrekidis, and M. K. Oberthaler, Phys. Rev. Lett. **107**, 193001 (2011).
[8] J.-Y. Zhang, S.-C. Ji, Z. Chen, L. Zhang, Z.-D. Du, B. Yan, G.-S. Pan, B. Zhao, Y.-J. Deng, H. Zhai, S. Chen, and J.-W. Pan, Phys. Rev. Lett. **109**, 115301 (2012).
[9] M. Egorov, B. Opanchuk, P. Drummond, B. V. Hall, P. Hannaford, and A. I. Sidorov, Phys. Rev. A **87**, 053614 (2013).
[10] T. Bienaimé, E. Fava, G. Colzi, C. Mordini, S. Serafini, C. Qu, S. Stringari, G. Lamporesi, and G. Ferrari, Phys. Rev. A **94**, 063652 (2016).
[11] E. Fava, T. Bienaimé, C. Mordini, G. Colzi, C. Qu, S. Stringari, G. Lamporesi, and G. Ferrari, Phys. Rev. Lett. **120**, 170401 (2018).
[12] See, e.g., J. Voit, Rep. Prog. Phys. **58**, 977 (1994).
[13] A. Recati, P. O. Fedichev, W. Zwerger, and P. Zoller, Phys. Rev. Lett. **90**, 020401 (2003).
[14] A. Recati, P. O. Fedichev, W. Zwerger, and P. Zoller, J. Opt. B **5**, S55 (2003).
[15] T. Stöferle, H. Moritz, C. Schori, M. Köhl, and T. Esslinger, Phys. Rev. Lett. **92**, 130403 (2004).
[16] B. Paredes, A. Widera, V. Murg, O. Mandel, S. Fölling, I. Cirac, G. V. Shlyapnikov, T. W. Hänsch, and I. Bloch, Nature (London) **429**, 277 (2004).
[17] T. Kinoshita, T. Wenger, and D. S. Weiss, Science **305**, 1125 (2004).
[18] E. Haller, M. Gustavsson, M. J. Mark, J. G. Danzl, R. Hart, G. Pupillo, and H.-C. Nägerl, Science **325**, 1224 (2009).
[19] A. F. Andreev and E. P. Bashkin, Sov. Phys. JETP **42**, 164 (1975).
[20] See, for instance, G. Ahlers, in *The Physics of Liquid and Solid Helium*, Part I, edited by K. H. Benneman and J. B. Ketterson (Wiley, New York, 1976).
[21] D. V. Fil and S. I. Shevchenko, Phys. Rev. A **72**, 013616 (2005).
[22] V. M. Kaurov, A. B. Kuklov, and A. E. Meyerovich, Phys. Rev. Lett. **95**, 090403 (2005).
[23] J. Nespolo, G. E. Astrakharchik, and A. Recati, New J. Phys. **19**, 125005 (2017).
[24] E. H. Lieb and W. Liniger, Phys. Rev. **130**, 1605 (1963).
[25] M. Girardeau, J. Math. Phys. (N. Y.) **1**, 516 (1960).
[26] Y.-Q. Li, S.-J. Gu, Z.-J. Ying, and U. Eckern, Europhys. Lett. **61**, 368 (2003).
[27] K. Yang and Y.-Q. Li, Int. J. Mod. Phys. B **17**, 1027 (2003).
[28] C. N. Yang, Phys. Rev. Lett. **19**, 1312 (1967).
[29] M. Gaudin, Phys. Lett. **24A**, 55 (1967).
[30] L. Parisi and S. Giorgini, Phys. Rev. A **95**, 023619 (2017).
[31] F. Grusdt, G. E. Astrakharchik, and E. A. Demler, New J. Phys. **19**, 103035 (2017).
[32] B. L. Hammond, W. A. Lester Jr., and P. J. Reynolds, *Monte Carlo Methods in Ab Initio Quantum Chemistry* (World Scientific, Singapore, 1994).
[33] See Supplemental Material at http://link.aps.org/supplemental/10.1103/PhysRevLett.121.025302 for more details on the guiding function.
[34] G. E. Astrakharchik and S. Giorgini, Phys. Rev. A **68**, 031602(R) (2003).
[35] L. Pitaevskii and S. Stringari, *Bose-Einstein Condensation and Superfluidity* (Oxford University Press, New York, 2016), Sec. 21.1.
[36] The instability is triggered by long-wavelength fluctuations of the magnetization density which are inhibited in our finite-size simulations. This allows for a reliable determination of the equation of state in the metastable regime at least when $\tilde{g}$ is only slightly larger than g.
[37] H. Shiba, Phys. Rev. B **6**, 930 (1972).
[38] M. T. Batchelor, M. Bortz, X.-W. Guan, and N. Oelkers, J. Phys. Conf. Ser. **42**, 5 (2006).
[39] X.-W. Guan and Z.-Q. Ma, Phys. Rev. B **85**, 033632 (2012).
[40] We solve the coupled integral equations of the Yang-Gaudin model for polarizations $P \gtrsim 10^{-3}$ and we thereby determine the susceptibility χ at small but still finite polarization. Because of logarithmic singularities [41,42], the calculation of χ at zero polarization would require much smaller values of P which cannot be reproduced by our numerical methods and are most likely experimentally irrelevant. We notice that this zero-polarization susceptibility satisfies the exact relation [43] $\chi v_s = [2/(\hbar\pi)]$ in terms of the spin velocity v_s and differs from the one shown in Fig. 2.

[41] P. Schlottmann, Int. J. Mod. Phys. **11**, 355 (1997).

[42] V. A. Zyuzin and D. L. Maslov, Phys. Rev. B **91**, 081102(R) (2015).

[43] C. F. Coll, Phys. Rev. B **9**, 2150 (1974).

[44] See Supplemental Material at http://link.aps.org/supplemental/10.1103/PhysRevLett.121.025302 for more details on the spin-dependent dynamic structure factor and its energy moments.

[45] D. Pines and P. Nozieres, *Theory of Quantum Liquids* (Benjamin, New York, 1966), Vol. 1.

[46] F. Dalfovo and S. Stringari, Phys. Rev. Lett. **63**, 532 (1989).

[47] We notice that the energy-weighted moment (f-sum rule) $m_1 = N[(\hbar^2 q^2)/(2m)]$ is not exhausted at low momenta by the spin-wave excitation. In fact, its contribution to the sum rule is suppressed by the drag effect and is given by $(m_1)_{sw} = m_1\{1 - [(4\rho_D)/\rho]\}$.

[48] See Supplemental Material at http://link.aps.org/supplemental/10.1103/PhysRevLett.121.025302 for a discussion of the sum rules which includes Refs. [45,46,49,50].

[49] L. Reatto and G. V. Chester, Phys. Rev. **155**, 88 (1967).

[50] P. C. Hohenberg and W. F. Brinkman, Phys. Rev. B **10**, 128 (1974).